Holocene African droughts relate to eastern equatorial Atlantic cooling

Syee Weldeab* Deutsche Forschungsgemeinschaft (DFG) Research Center Ocean Margins, Bremen University, Leobener Strasse, 28359 Bremen, Germany
Ralph R. Schneider Institut für Geowissenschaften, Universität Kiel, Ludewig-Meyn-Strasse 10, 24118 Kiel, Germany
Martin Kölling, Gerold Wefer Deutsche Forschungsgemeinschaft (DFG) Research Center Ocean Margins, Bremen University, Leobener Strasse, 28359 Bremen, Germany

ABSTRACT

Here we present evidence that the Holocene African monsoon system (AMS) varied in response to the eastern equatorial Atlantic sea-surface temperature (SST). Several short-term episodes of decreased moisture availability as a result of low eastern equatorial Atlantic SST are suggested by planktonic foraminiferal Mg/Ca ratios. These episodes promoted a weakening of the AMS and thus determined the timing and intensity of arid periods. Local sea-surface salinities also reveal regional patterns of precipitation in equatorial western Africa. The high eastern equatorial Atlantic SSTs occur in concert with seasonally increased insolation at low latitudes, suggesting a strong response of African monsoonal precipitation to oceanic conditions at low latitudes.

Keywords: eastern equatorial Atlantic, Mg/Ca, sea-surface temperature, African monsoon, aridity, lake levels.

INTRODUCTION

Holocene terrestrial records (Gasse, 2000; Gasse and Van Campo, 1994) from western, central, eastern, and northern Africa reveal a recurring alternation of arid and humid phases associated with weakening and strengthening of the African monsoon system (AMS). The periods of drought likely brought about environmental hardship, triggering population migration, giving rise to changes in the modes of agricultural production, and influencing the fall or rise of civilizations (deMenocal, 2001; Haug et al., 2003; Weiss, 2000). However, discrepancies exist with respect to the timing and severity of the recurring droughts owing to the discontinuity of continental climatic records, site-specific features resulting in uncertainties in intersite correlation, and the asynchronous response of terrestrial ecosystems to marine signals (Gasse, 2000, 2002; Jennerjahn et al., 2004). Moreover, a lack of climate records from the eastern equatorial Atlantic, to which the AMS is coupled (Camberlin et al., 2001), represents a drawback for deducing oceanic-atmospheric feedback mechanisms that probably controlled AMS variability. The seasonality of African monsoon precipitation is governed by the location of maximum solar heating, the migration of the intertropical convergence zone (ITCZ), and the dipole behavior between the northern and southern Atlantic sea-surface temperatures (SST) (Nicholson and Flohn, 1980). Among these factors, eastern equatorial Atlantic SST variability is one determining factor for AMS moisture availability (Camberlin et al., 2001; Fontaine and Bigot, 1993). Thus, a better knowledge of the SSTs in the eastern equatorial Atlantic is pivotal for the understanding of Holocene variations in African monsoonal precipitation. Here we present SSTs and variations in the ice-volume-free oxygen isotope composition of seawater ($\delta^{18}O_{sw}$), a proxy for local hydrological change (i.e., salinity), from the eastern equatorial Atlantic.

MATERIAL AND METHODS

Core GeoB4905-4 was retrieved from the eastern equatorial Atlantic (02°30.0′N, 09°23.04′E; water depth 1328 m) off Cameroon near the Sanaga and Nyong Rivers. Modern seasonal sea-surface salinity (SSS) variation at the core site is controlled by freshwater discharge of the Sanaga and Nyong Rivers that drain an area of 158,000 km^2, with a mean annual discharge volume of 77 km^3, into the Gulf of Guinea (Global Runoff Data Center, 2005). At the core site, the average SSS value at 0–20 m water depth (Levitus and Boyer, 1994) continuously decreases from 31‰ (August) to 27.5‰ (December), reflecting the highest riverine discharge between mid-July and November (GSA Data Repository[1]).

During periods of low riverine discharge (February–July), the SSS steadily increases from 28‰ (February) to 31.5‰ (July). The chronology of the core is based on 12 AMS datings conducted at the Leibnitz Labor (University of Kiel, Germany), using monospecific (*Globigerinoides ruber* pink) and mixed planktonic foraminifers. For the conversion of the ^{14}C dates to calendar age, CALIB version 5.01 (Stuiver and Reimer, 1993) and the Marine04 Data Set were used (Table DR1). The complete data set covers the past 21 k.y. (calendar years). Reconstruction of SST and $\delta^{18}O_{sw}$ is based on Mg/Ca ratios and $\delta^{18}O$ of the shallow-dwelling planktonic foraminifer *G. ruber* pink variety, respectively.

Cleaning the *G. ruber* tests for the Mg/Ca measurements followed the protocol used by Martin and Lea (2002), but omitted the diethylenetriaminepenta-acetate (DTPA) chelation step. The Mg/Ca measurements were conducted on an inductively coupled plasma–optical emission spectrometer. For details on the sample preparation and analytical procedure, see the GSA Data Repository (see footnote 1). Standards and replicate analyses of samples show the mean reproducibility as $<\pm0.05$ Mg/Ca mmol/mol.

The variation of $\delta^{18}O_{sw}$ was reconstructed by subtracting the influence of temperature (Shackleton, 1974) and global ice-volume effect (Fairbanks, 1989) on the $\delta^{18}O$ composition of *G. ruber* pink. Taking into account that the analytical error of Mg/Ca and the error related to translation Mg/Ca in the Mg/Ca SST estimation is $\sim\pm1.2$ °C, corresponding to ±0.24‰ $\delta^{18}O$ and an analytical error of $\delta^{18}O$ ±0.05, the resulting error in the $\delta^{18}O_{sw}$ estimation is $\sim\pm0.29$‰. To provide a rough estimate for the implied range of salinity change, SSS was calculated using the $\delta^{18}O_{sw}$-SSS relationship (see GSA Data Repository) in the eastern low-latitude Atlantic (Wang et al., 1995). The error estimation of calculated SSS accounts for ±0.7‰.

RESULTS AND DISCUSSION

Our SST estimates show that the late part (19–20 ka) of the Last Glacial Maximum (LGM, 19–23 ka; Mix et al., 2001) was cooler by 4 °C in comparison to the mid-Holocene temperature optimum (Fig.

*Current address: Department of Geological Sciences and Marine Science Institute, University of California–Santa Barbara, Santa Barbara, California 93106-9630, USA.

[1]GSA Data Repository item 2005189, sample preparation and analysis of Mg/Ca, Figures DR1 and DR2, and Tables DR1 and DR2, is available online at www.geosociety.org/pubs/ft2005.htm, or on request from editing@geosociety.org or Documents Secretary, GSA, P.O. Box 9140, Boulder, CO 80301-9140, USA.

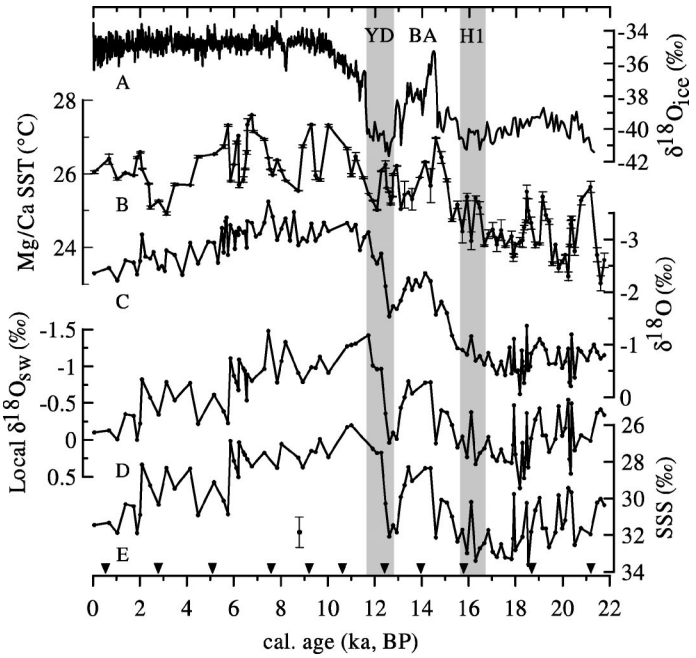

Figure 1. Eastern equatorial Atlantic climate records and Greenland Ice Sheet Project 2 (GISP2) ice record from Greenland. A: $\delta^{18}O_{ice}$ (‰ vs. standard mean ocean water SMOW) of GISP2 (Grootes et al., 1993). B: Mg/Ca sea-surface temperature (SST) record (*Globigerinoides ruber* pink; test size, 250–300 μm) in eastern equatorial Atlantic from core GeoB4905-4, retrieved in 1328 m water depth off Cameroon. For Mg/Ca-based SST estimation, we applied relationship developed by Anand et al. (2003): Mg/Ca(mmol/mol) = 0.38exp[0.09 × *T*(°C)]. Line traces mean of three replicate analyses, and vertical lines show standard deviation of replicates. C: $\delta^{18}O$ record (‰ vs. Peedee belemnite, PDB) of *G. ruber* pink from core GeoB4905-4 (Adegbie et al., 2003). D: Ice-volume-free local $\delta^{18}O_{sw}$ (‰ vs. SMOW) variation in eastern equatorial Atlantic from core GeoB4905-4 as proxy for sea-surface salinity (SSS). E: SSS calculated using $\delta^{18}O_{sw}$-SST-SSS relationship suggested for eastern low-latitude Atlantic (Wang et al., 1995). Uncertainties related to SSS calculation account for ±0.7‰ (vertical line). YD—Younger Dryas; H1—Heinrich event 1; BA—Bølling-Allerød; gray shading indicates time intervals of these events. Triangles at bottom indicate age control points in age model of core GeoB4905-4 (Table DR1 in GSA Data Repository; see footnote 1).

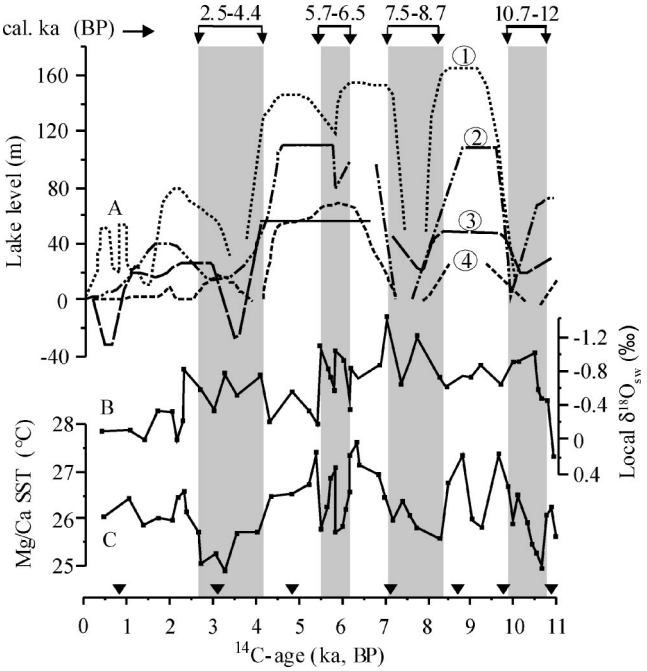

Figure 2. Correlation of Holocene eastern equatorial Atlantic sea-surface temperature (SST) and local $\delta^{18}O_{sw}$ with African lake-level fluctuations. A: African lake-level fluctuations during Holocene, redrawn from Gasse (2000): 1, Lake Abhè; 2, Ziway-Shala lake system; 3, Lake Bosumtwi; 4, Bahr-el-Ghazal. Present lake level is shown as 0 m. B: Local $\delta^{18}O_{sw}$ variation. C: eastern equatorial Atlantic SST (see also Fig. 1B). Gray bars show correlation of low eastern equatorial Atlantic SST, increased local $\delta^{18}O_{sw}$, and low lake level. Bottom axis: triangles indicate age control points in age model. Note that chronology is given in ^{14}C age (ka) and is not corrected for reservoir effect. Top axis: age ranges of gray-shaded intervals.

1B). This agrees with evidence (Guilderson et al., 1994; Rühlemann et al., 1999; Visser et al., 2003) that the tropical ocean during the LGM was colder by 3–5 °C than during the Holocene. For the time intervals corresponding to abrupt and pronounced cold phases in the North Atlantic, the Heinrich event 1 and the Younger Dryas (Bond et al., 1993; Grootes et al., 1993), the eastern equatorial Atlantic record indicates a slight warming trend. Small-scale temperature variations superimposed on the warming trend make the exact timing of warming in the tropical ocean with respect to the Heinrich event 1 and the Younger Dryas difficult. According to our age model, the $\delta^{18}O$ record implies that a drastic hydrological change in the catchment area coinciding with the Younger Dryas cold interval in the northern high latitudes had already started ca. 12.5 ka (Figs. 1B–1D). Cold northern subtropical and mid-latitude SSTs during the Younger Dryas (Bard et al, 2000; Zhao et al., 1995) and associated atmospheric configurations (weakening of low-pressure cells and westerlies) over northern Africa may have fostered seasonally prolonged positioning of the ITCZ at its southernmost location, resulting in enhanced precipitation in the catchment area. Slight eastern equatorial Atlantic warming during the Heinrich event 1 and Younger Dryas might have been associated with reduced heat exchange between the tropical Atlantic and the northern high latitudes (Rühlemann et al., 1999).

Unlike the Greenland $\delta^{18}O_{ice}$ record, the Holocene interval of the eastern equatorial Atlantic SST record indicates pronounced millennial- and centennial-scale temperature variations (Fig. 1B). Eastern equatorial Atlantic warming started ca. 12 ka and continued until 9 ka, reaching a temperature of ~27 °C. This warming was followed by a cooling trend that started ca. 8.7 ka and terminated ca. 7.5 ka. The SST then increased again until 6.7 ka, showing maximum Holocene SST values of ~27.5 °C. Afterward, a gradual cooling began that ended at 2.5 ka, with the lowest Holocene SST values, ~25 °C, between 3.0 and 2.5 ka. Superimposed on these millennial-scale cooling and warming patterns, several short (centennial scale) cold phases are revealed by the SST record; i.e., during the intervals 9.7–9.2, 6.6–6.3, and 6.0–5.7 ka. Following a rapid SST rise at 2 ka, a less pronounced SST decrease is indicated for the period from 1.7 to 1.0 ka.

Calculated ice-volume-free $\delta^{18}O_{sw}$ variations and $\delta^{18}O$ of *G. ruber* show nearly identical trends, implying that the oxygen isotope signal is controlled mainly by variations of freshwater discharge (Figs. 1C, 1D), thus reflecting SSS variations (Fig. 1E). The highest $\delta^{18}O_{sw}$ values (corresponding to the highest salinity) were observed for the period between 15.5 and 18.0 ka, whereas values in the latter part of the LGM (19–20 ka), when coldest SSTs prevailed, were slightly lower. Concomitant to the onset of the Bølling-Allerød interval, a gradual $\delta^{18}O_{sw}$ decrease began and reached the lowest pre-Holocene values of ~−0.75‰ between 13.5 and 14.5 ka. Before the onset of the Younger Dryas, a $\delta^{18}O_{sw}$ increase resumed and peaked at ~0.2‰ at 12.5 ka. The $\delta^{18}O_{sw}$ rapidly declined to the lowest Holocene values of ~−1.75‰ ca. 11.5 ka (Figs. 1C and 2C). This $\delta^{18}O_{sw}$ minimum was followed by a continuous rise throughout the Holocene that ended at values of ~−0.13‰. This general trend toward modern values after

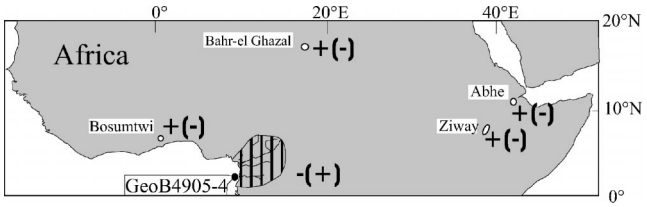

Figure 3. Relationship of eastern equatorial Atlantic sea-surface temperature (SST) to precipitation in catchment areas of lakes and Sanaga and Nyong Rivers, deduced from lake-level fluctuations (Gasse, 2000) and local $\delta^{18}O_{sw}$ (sea-surface salinity, SSS) variation, respectively. +(−)—correlation of increased eastern equatorial Atlantic SST and high lake levels and decreased eastern equatorial Atlantic SST and low lake levels; −(+)—correlation of decreased eastern equatorial Atlantic SST and high precipitation, and increased SST and low precipitation, in riverine catchment areas of Sanaga and Nyong Rivers; GeoB4905-4—core retrieved from eastern equatorial Atlantic in 1328 m water depth. See also supporting material in GSA Data Repository (see footnote 1).

the early Holocene salinity minimum is marked by moderate amplitude variations at 8–7.5, 6.5–6, and 4–2 ka, with modern values of local $\delta^{18}O_{sw}$ established during the past 0.6 k.y.

Taking into account the dating uncertainties for both marine and terrestrial records, and despite the regional nature of climate proxy records (Gasse, 2000, 2002; Gasse and Van Campo, 1994), the millennial-scale Holocene cold periods in the eastern equatorial Atlantic concur with low levels of several African lakes for the intervals 12–10.7, 8.7–7.5, 6.5–5.7, and 4.4–2.5 ka, and thus with arid conditions in western Africa, the Sudano-Sahelian region, and eastern Africa (Figs. 2 and 3). Periods of high eastern equatorial Atlantic SST correspond to the pronounced humid phases. Centennial-scale eastern equatorial Atlantic SST cold phases at the time intervals 6.5–5.7 and 9.6–9.2 ka, which lasted ~250 and 400 yr, are not concurrent with lake-level falls in Lake Bosumtwi and Bahr-el Ghazal (Fig. 2), whereas in Lake Abhè and Ziway-Shala (eastern Africa) a weakly pronounced drop in lake level at 6.5–5.7 ka was reconstructed (Gasse, 2000). This may indicate that available Holocene lake-level reconstructions are still insufficient to reveal all centennial-scale fluctuations, whereas, in contrast, our comparison strongly supports the close link between eastern equatorial Atlantic SST variations and monsoonal precipitation over the whole of northern Africa at millennial time scales.

The reconstructed ice-volume-free $\delta^{18}O_{sw}$ variations are assumed to reflect changes in freshwater discharge of the Sanaga and Nyong Rivers, and hence the precipitation history of mainly equatorial western Africa. Rather than closely covarying with eastern equatorial Atlantic SST millennial-scale variations such as the north African lake-level fluctuations, $\delta^{18}O_{sw}$ changes off the Sanaga and Nyong Rivers exhibit stepwise increases toward higher salinities during the course of the Holocene (Fig. 2B), indicating long-term development of decreasing precipitation in the catchment area. This long-term $\delta^{18}O_{sw}$ pattern may be related to the Holocene evolution of the solar radiation in the Northern Hemisphere (Berger, 1978) and its impact on the hydrological cycle. Superimposed on the long-term trend, there is also the tendency for cold eastern equatorial Atlantic SSTs to correlate with periods of relatively low $\delta^{18}O_{sw}$ and therefore with high precipitation over equatorial western Africa. Moreover, the comparison of the Holocene eastern equatorial Atlantic $\delta^{18}O_{sw}$ variations to north African lake-level fluctuations (Fig. 2) suggests an inverse relationship between precipitation changes over northern and equatorial western Africa with respect to eastern equatorial Atlantic SST variations. Low $\delta^{18}O_{sw}$, associated with enhanced freshwater discharge and intense precipitation in the equatorial drainage area, is contemporaneous with low lake levels and reduced monsoonal precipitation north of 6°N, whereas periods of relatively high $\delta^{18}O_{sw}$ correlate with higher lake levels. Considering age model uncertainties, our finding is consistent with freshwater diatom records (Nguetsop et al., 2004) from lakes within the catchment basin of the Sanaga River, indicating high lake levels at times of low $\delta^{18}O_{sw}$. In contrast to our salinity reconstruction and the diatom record (Nguetsop et al., 2004), however, the pollen record from lakes within the catchment area of the Sanaga River (Elenga et al., 2005) indicates a forest minimum between 2.8 and 2 ka. The cause for this discrepancy may lie in the loosely defined catchment area of the pollen record, while the riverine discharge affecting the salinity of our core site stems from a relatively well defined catchment basin. Therefore, considering the different oceanic and terrestrial evidence for Holocene precipitation changes, a precipitation response pattern emerges, implying that reduced precipitation prevailed over equatorial western Africa during the Holocene, contemporaneous with more humid conditions north of 6°N, with a longitudinal extent from 0° to ~40°E. Conversely, relatively humid conditions over equatorial western Africa occurred together with more arid periods in northern Africa associated with low eastern equatorial Atlantic SST.

Concordant with the Holocene eastern equatorial Atlantic SST and precipitation increases over northern Africa (Fig. 3), modeling results (Liu et al., 2003) revealed low-latitude mean annual insolation increases. Furthermore, an increase in the seasonal cycle of incoming solar radiation and the resulting seasonally enhanced cycle of surface temperature, which has more relevance for the monsoon intensity, has been suggested by several modeling studies for the time intervals of ~6 k.y. (Braconnot et al., 2000; Ganopolski et al., 1998; Hewitt and Mitchell, 1998; Kutzbach and Liu, 1997) and 9 k.y. (Kutzbach and Gallimore, 1988). According to modeling studies (Braconnot et al., 2000; Ganopolski et al., 1998), in contrast to land-surface temperatures, a delayed response of equatorial SST to seasonally increased insolation forcing leads to an increased land-ocean temperature gradient and earlier northward movement of the ITCZ, whereas decreased planetary albedo owing to a reduced subtropical desert (Ganopolski et al., 1998), causing a further increase in the land-surface temperature, delayed the seasonal retreat of the ITCZ to its southernmost position. This gave rise to prolonged monsoonal rainfall in northern Africa and likely reduced precipitation in areas close to the Gulf of Guinea. This is consistent with our $\delta^{18}O_{sw}$ records, which indicate slightly reduced riverine discharge and hence reduced precipitation in the catchment area concordant with humid phases in northern Africa.

This dipolar precipitation pattern between the coastal areas of the Gulf of Guinea and northern Africa is consistent with instrumental data and modeling studies (Braconnot et al., 2000; Camberlin et al., 2001; Fontaine and Bigot, 1993; Giannini et al., 2003; Rowell et al., 1995). Complex interplay involving localized cyclonic circulation and the influence of southern Atlantic SST and El Niño Southern Oscillation activities have been suggested as factors that have influenced interannual and interdecadal precipitation variability in areas close to the Gulf of Guinea (Braconnot et al., 2000; Camberlin et al., 2001; Fontaine and Bigot, 1993). However, millennial-scale changes in seasonal solar radiation and the associated land-ocean temperature gradient enhanced moisture availability owing to surface ocean warming (and reduced moisture availability due to surface ocean cooling), and vegetation feedback mechanisms likely governed the Holocene monsoon variability.

CONCLUSIONS

Our SST records and the terrestrial records suggest that insolation-forced SST conditions in the eastern equatorial Atlantic Ocean profoundly affect the hydrological cycle of the African monsoon system. Delayed response of the surface ocean to seasonally increased insolation forcing and vegetation feedback may have increased the land-ocean temperature gradient, allowing earlier northward displacement

and delayed retreat of the ITCZ, respectively, hence enabling the penetration of moist air masses deep into the African continent and strengthening prolonged monsoonal precipitation. Although increased eastern equatorial Atlantic SST fostered moisture availability in northern Africa, the prolonged stay of the ITCZ at its northernmost position may have resulted in a relative reduction of precipitation in the area of equatorial western Africa.

The correlation of decreased (increased) eastern equatorial Atlantic SST with low (high) lake-level records from eastern Africa, which is equally influenced by moisture advection from the tropical Atlantic and the equatorial Indian Ocean, supports insolation-induced cooling (warming) of the equatorial oceans. However, a high-resolution record from the eastern equatorial Indian Ocean is needed to corroborate this hypothesis.

ACKNOWLEDGMENTS

We thank W. Hale for improving the English, S. Hessler for technical assistance, and James Scourse and J.-B. Stuut for helpful discussions. The helpful comments of R. Thunell, T. Guilderson and other reviewers are gratefully acknowledged. This study was supported by the European Community, contract EVR1-CT-2001-40018 (CESOP). This is Research Center Ocean Margins publication RCOM0316.

REFERENCES CITED

Adegbie, A.T., Schneider, R., Röhl, U., and Wefer, G., 2003, Glacial millennial-scale fluctuation in central African precipitation recorded in terrigenous sediment supply and fresh water signals offshore Cameroon: Palaeogeography, Palaeoclimatology, Palaeoecology, v. 197, p. 323–333, doi: 10.1016/S0031-0182(03)00474-7.

Anand, P., Elderfield, H., and Conte, M.H., 2003, Calibration of Mg/Ca thermometry in planktonic foraminifera from a sediment trap time series: Paleoceanography, v. 18, p. 1050, doi: 10.1029/2002PA000846.

Bard, E., Rostek, F., Turon, J.-L., and Gendreau, S., 2000, Hydrological impact of Heinrich events in the subtropical Northeast Atlantic: Science, v. 289, p. 1321–1323, doi: 10.1126/science.289.5483.1321.

Berger, A., 1978, Long-term variations of caloric insolation resulting from the Earth's orbital elements: Quaternary Research, v. 9, p. 139–167.

Bond, G., Broecker, W., Johnsen, S., McManus, J., Labeyrie, L., Jouzel, J., and Bonani, G., 1993, Correlations between climate records from North Atlantic sediments and Greenland ice: Nature, v. 365, p. 143–147, doi: 10.1038/365143a0.

Braconnot, P., Marti, O., Joussaume, S., and Leclaince, Y., 2000, Ocean feedback in response to 6 kyr BP insolation: Journal of Climate, v. 13, p. 1537–1553, doi: 10.1175/1520-0442(2000)013<1537:OFIRTK>2.0.CO;2.

Camberlin, P., Janicot, S., and Poccard, I., 2001, Seasonality and atmospheric dynamics of the teleconnection between African rainfall and tropical sea surface temperature: Atlantic vs. ENSO: International Journal of Climatology, v. 21, p. 973–1005, doi: 10.1002/joc.673.

deMenocal, P.B., 2001, Cultural responses to climate change during the late Holocene: Science, v. 292, p. 667–673, doi: 10.1126/science.1059827.

Elenga, H., Maley, J., Vincens, E., and Farrera, I., 2005, Palaeoenvironments, palaeoclimates and landscape developments in Atlantic equatorial Africa: A review of key sites covering the last 25 kyrs, *in* Battarbee, W.R., et al., eds., Past climate variability through Europe and Africa, Volume 6: Development in palaeoevironmental research: Dordrecht, Springer, p. 181–198.

Fairbanks, R.G., 1989, A 17,000-year glacio-eustatic sea level record: Influence of glacial melting waters on the Younger Dryas event and deep-ocean circulation: Nature, v. 342, p. 637–642, doi: 10.1038/342637a0.

Fontaine, B., and Bigot, S., 1993, West African rainfall deficits and sea surface temperatures: International Journal of Climatology, v. 13, p. 271–285.

Ganopolski, A., Kubatzki, C., Clausen, M., Brovkin, V., and Petoukhov, V., 1998, The influence of vegetation-atmosphere-ocean on climate during the mid-Holocene: Science, v. 280, p. 1916–1919, doi: 10.1126/science.280.5371.1916.

Gasse, F., 2000, Hydrological changes in the African tropics since the Last Glacial Maximum: Quaternary Science Reviews, v. 19, p. 189–211, doi: 10.1016/S0277-3791(99)00061-X.

Gasse, F., 2002, Kilimanjaro's secrets revealed: Science, v. 298, p. 548, doi: 10.1126/science.1078561.

Gasse, F., and Van Campo, E., 1994, Abrupt post-glacial climate events in West Asia and North Africa monsoon domains: Earth and Planetary Science Letters, v. 126, p. 435–456, doi: 10.1016/0012-821X(94)90123-6.

Giannini, A., Saravanan, R., and Chang, P., 2003, Oceanic forcing of Sahel rainfall on interannual to interdecadal time scale: Science, v. 302, p. 1027–1030, doi: 10.1126/science.1089357.

Global Runoff Data Center, 2005, Global runoff data: Germany, http://grdc.bafg.de.

Grootes, P.M., Stuiver, M., White, J.W.C., Johnsen, S., and Jouzel, J., 1993, Comparison of oxygen isotope records from the GISP2 and GRIP Greenland ice cores: Nature, v. 366, p. 552–554, doi: 10.1038/366552a0.

Guilderson, T.P., Fairbanks, R.G., and Rubenstone, J.L., 1994, Tropical temperature variations since 20,000 years ago: Modulating interhemispheric climate change: Science, v. 263, p. 663–665.

Haug, G.H., Günther, D., Peterson, L.C., Sigman, D.M., Hughen, K.A., and Aeschlimann, B., 2003, Climate and the collapse of Maya civilization: Science, v. 299, p. 1731–1735, doi: 10.1126/science.1080444.

Hewitt, C., and Mitchell, J.F.B., 1998, A fully coupled GCM simulation of the climate of the mid-Holocene: Geophysical Research Letters, v. 25, p. 361–364, doi: 10.1029/97GL03721.

Jennerjahn, T., Ittekkot, V., Arz, H., Behling, H., Pätzold, J., and Wefer, G., 2004, Asynchrony of preserved terrestrial and marine signals of climate change in the tropics during the Heinrich events: Science, v. 306, p. 2236–2239, doi: 10.1126/science.1102490.

Kutzbach, J.E., and Gallimore, R.G., 1988, Sensitivity of a coupled atmosphere/mixed layer ocean model to changes in orbital forcing at 9000 years BP: Geophysical Research Letters, v. 93, p. 803–821.

Kutzbach, J.E., and Liu, Z., 1997, Response of the African monsoon to orbital forcing and ocean feedbacks in the middle Holocene: Science, v. 278, p. 440–443, doi: 10.1126/science.278.5337.440.

Levitus, S., and Boyer, T.P., 1994, World ocean atlas 1994 Volume 4: Temperature: NOAA Atlas NESDIS 4: Washington, D.C., U.S. Department of Commerce, 117 p.

Liu, Z., Bradly, E., and Lynch-Stieglitz, J., 2003, Global ocean response to orbital forcing in the Holocene: Paleoceanography, v. 18, 1041, doi: 10.1029/2002PA000819.

Martin, P.A., and Lea, D.W., 2002, A simple evaluation of cleaning procedures on fossil benthic foraminiferal Mg/Ca: Geochemistry Geophysics Geosystems, v. 3, 8401, doi: 10.1029/2001GC000280.

Mix, A.C., Bard, E., and Schneider, R., 2001, Environmental processes of the ice age: Land, oceans, glaciers (EPILOG): Quaternary Science Reviews, v. 20, p. 627–657, doi: 10.1016/S0277-3791(00)00145-1.

Nguetsop, V.F., Servant-Vildary, S., and Servant, M., 2004, Late Holocene climate change in West Africa, a high resolution diatom record from equatorial Cameroon: Quaternary Science Reviews, v. 23, p. 591–609, doi: 10.1016/j.quascirev.2003.10.007.

Nicholson, S.E., and Flohn, H., 1980, African environmental and climatic changes and the general atmospheric circulation in the late Pleistocene: Climatic Change, v. 2, p. 313–348, doi: 10.1007/BF00137203.

Rowell, D.P., Folland, C.K., and Maskel, K., 1995, Variability of summer rainfall over tropical North Africa (1906–92): Observation and modeling: Royal Meteorological Society Journal, v. 121, p. 669–704, doi: 10.1256/smsqj.52310.

Rühlemann, C., Mulitza, S., Müller, P.J., Wefer, G., and Zahn, R., 1999, Warming of the tropical Atlantic Ocean and slowdown of thermohaline circulation during the last deglaciation: Nature, v. 402, p. 511–514, doi: 10.1038/990069.

Shackleton, N.J., 1974, Attainment of isotopic equilibrium between ocean water and the benthonic foraminiferal genus *Uvigerina*: Isotopic changes in the ocean during the last glacial: Colloques Internationaux du Centre National de la Recherche Scientifique, v. 219, p. 203–209.

Stuiver, M., and Reimer, P.J., 1993, Extended 14C data-base and revised calib 3.0 C-14 age calibration program: Radiocarbon, v. 35, p. 215–230.

Visser, K., Thunell, R., and Stott, L., 2003, Magnitude and timing of temperature change in the Indo-Pacific warm pool during deglaciation: Nature, v. 421, p. 152–155, doi: 10.1038/nature01297.

Wang, L., Sarnthein, M., Duplessy, J.-C., Erlenkeuser, H., and Jung, S., 1995, Paleo sea surface salinities in the low-latitude Atlantic: The $\delta^{18}O$ record of *Globigerinoides ruber* (white): Paleoceangraphy, v. 10, p. 749–761, doi: 10.1029/95PA00577.

Weiss, H., 2000, Beyond the Younger Dryas, *in* Bawden, G., and Reycraft, R.M., eds., Environmental disaster and archaeology of human response: Albuquerque, Maxwell Museum of Anthropology, University of New Mexico, p. 75–95.

Zhao, M., Beveridge, N.A.S., Shackleton, N.J., Sarnthein, M., and Eglinton, G., 1995, Molecular stratigraphy of cores off northwest Africa: Sea surface temperature history over the last 80 kyr: Paleoceanography, v. 10, p. 661–675, doi: 10.1029/94PA03354.

Manuscript received 17 May 2005
Revised manuscript received 18 August 2005
Manuscript accepted 19 August 2005

Printed in USA